

Improved Fault Ride Through Capability in DFIG Based Wind Turbines Using Dynamic Voltage Restorer With Combined Feed-Forward and Feed-Back Control

RINI ANN JERIN AMALORPAVARAJ¹, (Student Member, IEEE),
PALANISAMY KALIANNAN¹, (Member, IEEE),
SANJEEVIKUMAR PADMANABAN², (Senior Member, IEEE),
UMASHANKAR SUBRAMANIAM¹, (Member, IEEE),
AND VIGNA K. RAMACHANDARAMURTHY³, (Senior Member, IEEE)

¹School of Electrical Engineering, VIT University, Vellore 632014, India

²Department of Electrical and Electronics Engineering, University of Johannesburg, Auckland Park, Johannesburg 2006, South Africa

³Power Quality Research Group, Universiti Tenaga Nasional 43009, Malaysia

Corresponding author: Rini Ann Jerin Amalorpavaraj (riniannjerin@gmail.com)

ABSTRACT This paper investigates the fault ride through (FRT) capability improvement of a doubly fed induction generator (DFIG)-based wind turbine using a dynamic voltage restorer (DVR). Series compensation of terminal voltage during fault conditions using DVR is carried out by injecting voltage at the point of common coupling to the grid voltage to maintain constant DFIG stator voltage. However, the control of the DVR is crucial in order to improve the FRT capability in the DFIG-based wind turbines. The combined feed-forward and feedback (CFFFB)-based voltage control of the DVR verifies good transient and steady-state responses. The improvement in performance of the DVR using CFFFB control compared with the conventional feed-forward control is observed in terms of voltage sag mitigation capability, active and reactive power support without tripping, dc-link voltage balancing, and fault current control. The advantage of utilizing this combined control is verified through MATLAB/Simulink-based simulation results using a 1.5-MW grid connected DFIG-based wind turbine. The results show good transient and steady-state response and good reactive power support during both balanced and unbalanced fault conditions.

INDEX TERMS Doubly-fed induction generator (DFIG), dynamic voltage restorer (DVR), fault ride-through (FRT), low voltage ride through (LVRT), combined feed forward feedback control.

I. INTRODUCTION

The boom in wind energy growth worldwide has led to a large penetration of wind energy into the power grid. This positive momentum of growth in wind power sector is very good news for climate change and clean energy developers [1]. Yet, for the grid operators, this large growth in wind energy was not a predicted phenomenon and therefore grid codes for grid integration of renewable energy were altered to make the renewable work in harmony with the grid. Among the new grid codes for grid integration of wind energy, Fault Ride Through (FRT) capability during transient conditions and reactive power control during steady-state conditions pose considerable challenges for variable speed wind turbines [2]. Wind farms are no longer allowed to disconnect during faults

and voltage sag conditions, instead are expected to operate like the conventional power plants, providing the reactive power support and to remain connected during system faults [3].

Doubly Fed Induction Generators (DFIG) are most popular among the wind turbines for their capability of decoupled active and reactive power control, partially scaled converters and variable speed operation [4]. Even though DFIG based wind turbines are the most dominant type of wind turbines, they are very sensitive to grid voltage disturbances. During the occurrence of fault, the voltage drops to zero and active power generation reduces, this leads to rapid increase in the rotor current in order to compensate the active power by the rotor side converter (RSC). Hence, the converter increases

the rotor voltage which leads to an overvoltage in the DC-link. Conventionally, crowbars are engaged to protect the power electronic converters from the flow of over-currents from the rotor. But during the operation of crowbar, the RSC is disabled and the rotor winding is short-circuited by shunt resistors [5]. Thereby the DFIG starts absorbing reactive power like an induction machine instead of offering reactive power support to the grid. In order to limit the flow of over-currents, other techniques are offered by crowbar in combination with DC-link chopper [6], Series Braking Resistor (SBR) [7], series R-L circuit [8] and STATCOM [9]. Several new methods are still being proposed to improve the FRT capability in DFIG based wind turbines. The updated grid code requirements established by Germany for FRT capability are shown in Fig. 1(a) and Fig. 1(b). The Figure 1(a) shows that for voltage sag the turbine should stay connected within the marked curve. And also the fault clearance should be at a gradient of 20% of the rated power per second. And the wind turbines should support the grid through reactive current support as shown in Figure 1(b) and that should take place within 20 ms after the fault occurrence [10].

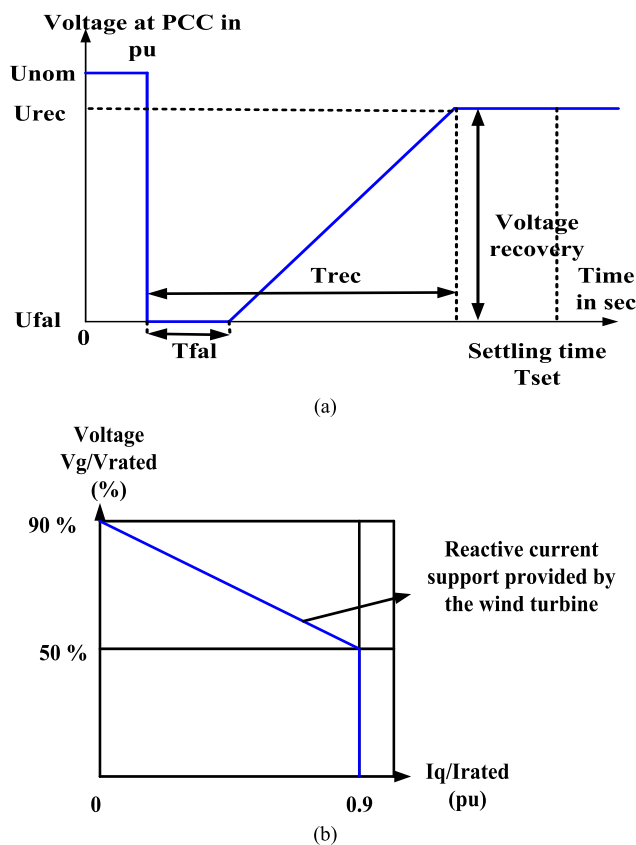


FIGURE 1. (a) Fault Ride Through grid code. (b) Reactive Power requirement grid code.

Static Synchronous Compensator (STATCOM) is a shunt compensation connected at the Point of Common Coupling (PCC) to provide high performance steady-state

and transient voltage control. But STATCOM cannot protect the Rotor Side Converter (RSC) of DFIG from the flow of over-currents and therefore require the assistance of crowbar [11]. STATCOM reduces the fault clearing time and provides the generator with increased decelerating torque when the voltage is recovered. This leads to an increase in the stability margin of the generator, but also increases the mechanical stress [12]. The application of a Dynamic Voltage Restorer (DVR) is a good solution as it does not require any other protective circuit during operation [13]. The general schematic diagram of the DVR connected to the DFIG is shown in Fig. 2. In comparison, DVR is more effective and direct solution for “restoring” the quality of voltage at its load-side terminals when the quality of voltage at its source-side terminals is disturbed [14]–[16].

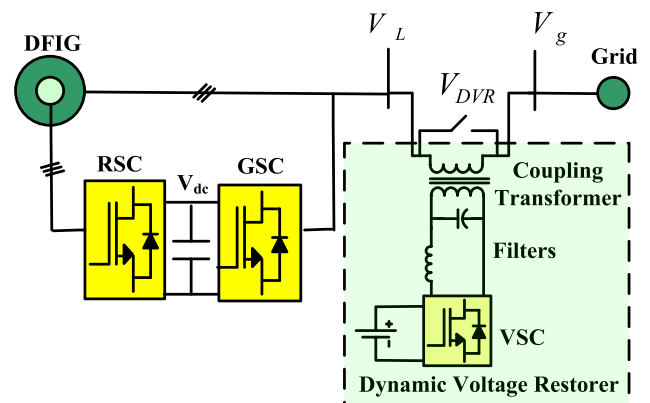


FIGURE 2. Schematic Diagram of DVR with DFIG.

The control algorithm utilized in the DVR for the FRT capability in DFIG determines the effectiveness of the solution to overcome most of the faults in the grid. The control of DVR is achieved in several steps and this includes detection, reference generation, voltage and current control and modulation [17]. When the reference voltage of the DVR is generated it can be directly applied for a modulator to generate the switching pulses for the VSI. This control scheme is known as a feed forward open loop control [18]–[20]. Although this control scheme has the advantages of simplicity and assured stability, it has poor transient response and may have steady state error due to voltage drop and phase shift on the series branch of the filter and injection transformer [21], [23], [24]. To overcome these problems feedback or combined feedback/feed-forward controllers are used [25]–[28]. In the feedback control system, the measured output voltage of the DVR (or load voltage) is fed back to a voltage controller.

This paper utilizes DVR with combined Feed-Forward and Feed-Back (CFFFB) control using voltage control based on PI controller. The improvement of FRT capability in DFIG based wind turbines using this CFFFB based DVR control is discussed in this paper for both balanced and unbalanced fault conditions. The remaining paper is structured as follows: Section 2 discusses the modeling of DFIG with DVR, Section 3 explains the DVR control, which

explains the voltage sag detection, load voltage reference generation and the operation of CFFFB control, Section 4 includes the simulation results and comparison of improvement in FRT capability using CFFFB control instead of a conventional Feed-Forward control and Section 5 ends with conclusion.

II. MODELING OF DFIG WIND TURBINE AND DVR

The understanding of the operation of DFIG during steady-state conditions and transient conditions are necessary to discuss about the control techniques to implement the FRT capability. The stator of DFIG wind turbine is connected directly to the grid and rotor is connected to the grid via slip rings through the RSC and GSC. The converter connected to the rotor side is the RSC and connected to the grid side is the GSC which together constitutes only up to 30-35% of the total capacity of the machine. Fig. 3 shows equivalent circuit of the DFIG.

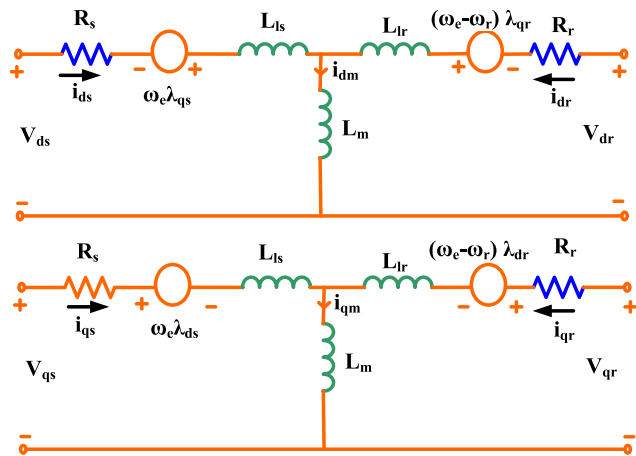


FIGURE 3. 'T-form' equivalent circuit of DFIG.

The stator and the rotor voltage in the synchronous dq reference frame are as given in Equation 1. The expressions of flux, voltages and currents are as in [15].

$$\begin{aligned}
 v_{ds} &= R_s i_{ds} + \frac{d\lambda_{ds}}{dt} - \omega_e \lambda_{qs} \\
 v_{qs} &= R_s i_{qs} + \frac{d\lambda_{qs}}{dt} + \omega_e \lambda_{ds} \\
 v_{dr} &= R_r i_{dr} + \frac{d\lambda_{dr}}{dt} - (\omega_e - \omega_r) \lambda_{qr} \\
 v_{qr} &= R_r i_{qr} + \frac{d\lambda_{qr}}{dt} + (\omega_e - \omega_r) \lambda_{dr}
 \end{aligned} \tag{1}$$

Here, v_{ds} , v_{qs} are dq stator voltages and v_{dr} , v_{qr} are dq rotor voltages. i_{ds} , i_{qs} are dq stator currents and i_{dr} , i_{qr} are dq rotor currents. ω_e is the supply angular frequency and ω_r is the rotor angular frequency. λ_{ds} , λ_{qs} are the dq stator flux linkages and λ_{dr} , λ_{qr} is the dq rotor flux linkages. R_s and R_r are the stator and rotor resistance respectively.

The L_s and L_r are the stator and rotor inductance respectively as given in Equation 2 and the flux linkages are given

in Equation 3.

$$\begin{aligned}
 L_s &= L_{ls} + L_m \\
 L_r &= L_{lr} + L_m
 \end{aligned} \tag{2}$$

L_{ls} and L_{lr} are the stator and rotor leakage inductance respectively and L_m is the magnetizing inductance.

$$\begin{aligned}
 \lambda_{ds} &= L_s i_{ds} + L_m i_{dr} \\
 \lambda_{qs} &= L_s i_{qs} + L_m i_{qr} \\
 \lambda_{dr} &= L_m i_{ds} + L_r i_{dr} \\
 \lambda_{qr} &= L_m i_{qs} + L_r i_{qr}
 \end{aligned} \tag{3}$$

In stator flux-oriented control, q-axis rotor current component controls the stator active power (P_s) and rotor d-axis current component controls the stator reactive power (Q_s) respectively are given in Eqn.4.

$$\begin{aligned}
 P_s &= \frac{3}{2} (v_{qs} i_{qs} + v_{ds} i_{ds}) \\
 Q_s &= \frac{3}{2} (v_{qs} i_{ds} - v_{ds} i_{qs})
 \end{aligned} \tag{4}$$

The threshold values of rotor current and DC-link voltage are essential to ensure efficient FRT capability. The threshold value of the rotor current during fault is 1.5 pu to 2 pu values. Also, the DC-link voltage rating is 1150 V and its threshold value is 1.35 pu [29]. The DVR operation should maintain the values of rotor current and DC-link voltage within these safety limits.

A. MODELING OF DYNAMIC VOLTAGE RESTORER (DVR)

The DVR is a voltage source converter connected in series to the grid and DFIG at PCC to inject the appropriate compensating voltage to correct the voltage sag, swell or harmonics and obtain the nominal stator voltage as shown in Fig. 2. The switching signals to voltage source converter are generated using PWM technique [30]. Conventional Phase locked loop (PLL) which is also in the synchronous dq reference frame detects the grid phase angle and utilized for synchronization. In-phase compensation method is utilized for both Feed-forward and CFFFB control of DVR as shown in Figure 4. Since, the grid codes demand compensation of full voltage sag during fault conditions, DVR is rated for the power of the wind turbine [31].

The power rating of DVR controlled by in-phase compensation method is as follows,

$$S_{DVR} = \sum_{k=a,b,c} V_{DVR,k}^{ref} * I_L \tag{5}$$

$V_{DVR,k}^{ref}$ is the rms of DVR injected voltage in phase k and I_L is the rms of load current.

The exchanged active power between DVR and grid is

$$P_{DVR} = P_L - P_g \tag{6}$$

$$= (3 * V_L * I_L * \cos) - \sum_{k=a,b,c} [V_{DVR,k}^{ref} * I_L * \cos \Psi]$$

$$V_{DVR,k}^{ref} = \sqrt{2} * |V_L - V_{g,k}^{ref}| \quad \text{and } k = a, b, c \tag{7}$$

Phase angle of injected voltage is the same as grid voltage.

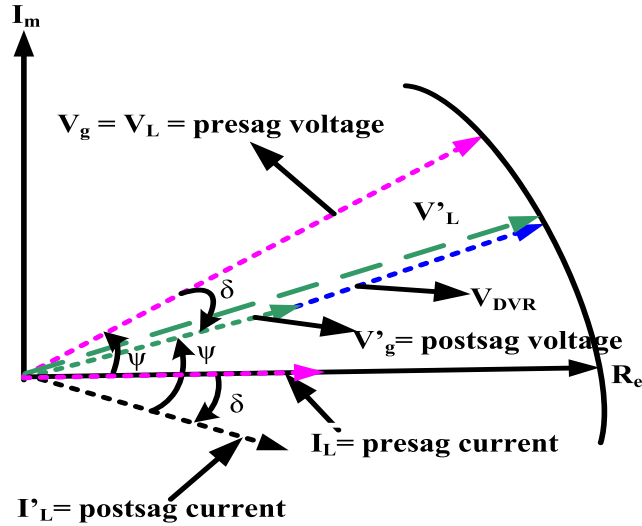


FIGURE 4. Compensation scheme of DVR based on in-phase compensation.

Ψ is the phase angle difference between load voltage and load current phasors, O is the phase jump of the grid voltage during the voltage sag, V_g is the grid voltage, V_L is the load voltage and I_L load current prior sag, V'_g is the grid voltage, V'_L is the load voltage and I'_L load current after sag, V_{DVR} is the DVR compensation voltage.

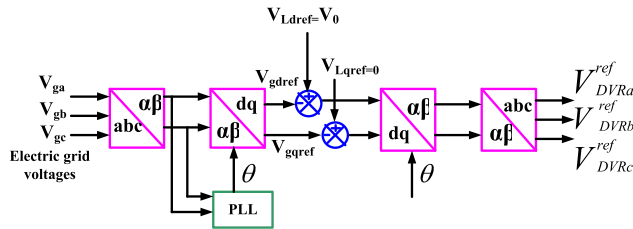


FIGURE 5. Feed forward control.

III. CONTROL TECHNIQUES OF DVR

A. FEED-FORWARD CONTROL STRATEGY

The operation of a conventional open-loop controller of DVR in synchronous reference frame [32], which is also called as a Feed-forward control is shown in Fig. 5. The $V_{Ldref} = V_0$ (where V_0 represents $(V_{La}^*, V_{Lb}^*, V_{Lc}^*)$), is the reference controlled by the required magnitude of the load bus voltage respectively.

$$\begin{aligned} V_{La}^* &= V_0 \sin \omega t \\ V_{Lb}^* &= V_0 \sin \left(\omega t - \frac{2\pi}{3} \right) \\ V_{Lc}^* &= V_0 \sin \left(\omega t + \frac{2\pi}{3} \right) \end{aligned} \quad (8)$$

The primary control structure depends on the supply voltage and its phase angle to calculate the required amplitude of compensation voltage. The operation of the control in the synchronous dq-reference frame allows simpler clamping of

the injection voltage. Therefore, enables DVR to partially compensate deep voltage sags and to maintain the sinusoidal injection voltage profile. The operation of control is synchronized to the supply voltage through Phase Locked Loop (PLL). The control generates the dq reference which is transformed to three phase stationary frame value in order to generate the PWM modulation signals [33], [34]. The compensation voltages are injected by the transformer to the grid at PCC.

B. COMBINED FEED-FORWARD AND FEED-BACK CONTROL STRATEGY

DVR control includes the detection of the start and end of the fault event, reference generation, transient and steady-state control of the injected voltage and the system protection. The Feed-Forward control includes the pre-sag voltage on the grid side before DVR to detect the voltage sag during fault. The Feed-Back control monitors the voltage mitigation on the DFIG side after DVR. The DC-link voltage is monitored for converter protection [35], [36]. This combined control includes the feedback which will take into account the voltage drop across the filter inductor and transformer [37].

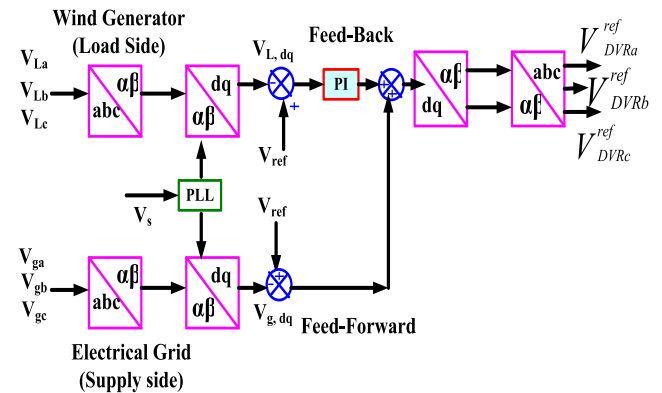


FIGURE 6. Control Scheme of DVR using combined Feed-Forward and Feed-Back control.

Voltage sag detection is an important part of the control which requires fast detection of voltage sag during fault conditions. The balanced and unbalanced sag is determined along with the phase jump. The load voltage references are generated by PLL to create sinusoidal load voltage references. These references are utilized for the dq co-ordinates of the controller. The PLL response is expected to be slow in order to avoid sudden changes in the phase angle. Combine Feed-Forward and Feed-Back control is a combination of electrical grid and load voltage respectively. Transient response based on the DC-link voltage is carried out by the Feed-Forward control to calculate the sag depth. But since Feed-Forward does not take into account the drop across the filters and series injection transformer, the Feed-Back control is utilized for closed loop load voltage Feed-Back to avoid steady-state errors. The control diagram of the combined Feed-Forward and Feed-Back control is shown in Fig. 6.

TABLE 1. Simulation parameters for DFIG and DVR.

| Symbol | Quantity | Values and units |
|------------|-----------------------------|------------------|
| P_{DFIG} | Rated power of DFIG | 1.5 MW |
| | Cut-in speed, cut-out speed | 3 m/s, 20 m/s |
| w_s | Rated wind speed | 11 m/s |
| V_s, f | Stator voltage/frequency | 575 V/ 50 Hz |
| R_s | Stator resistance | 0.023 pu |
| R_r | Rotor resistance | 0.016 pu |
| L_{ls} | Stator leakage inductance | 0.18 pu |
| L_{lr} | Rotor leakage inductance | 0.16 pu |
| H | Generator inertia constant | 0.685 |
| V_{dc} | Nominal DC bus voltage | 1150 V |
| | Converter rating | 30 % |
| P_{DVR} | DVR capacity | 1.5 MVA |
| L_{DVR} | DVR Filter inductance | 0.1 mH |
| C_{DVR} | DVR Filter capacitance | 1 μ F |
| f_{DVR} | DVR Switching frequency | 10 kHz |
| | DC-link voltage | 300 V |
| | Series transformer ratio | 1:1 |

IV. SIMULATION RESULTS AND DISCUSSION

The simulation results during balanced and unbalanced fault conditions using DVR are discussed. The results of transient active power control, reactive power support, transient voltage control, speed control, fault current control of RSC and GSC, DC-link voltage control and harmonics performance in terms of %THD are discussed in detail during various fault conditions. The test system is simulated for DFIG of 1.5 MW wind turbine connected to electrical grid in MATLAB/Simulink environment. The simulation parameters of the DFIG and DVR are given in Table 1. The FRT performance is evaluated for balanced and unbalanced sag of 35 % which lasts for 5 cycles between 0.7 s to 0.8 s, short-circuit fault and harmonics. The FRT performance of the wind turbine is evaluated and analyzed for the following cases:

- Case 1: Balanced sag of 0.35 pu
- Case 2: Unbalanced sag of 0.35 pu (single line to ground fault, 1LG)
- Case 3: Short-circuit fault (three lines to ground fault, 3LG)
- Case 4: Harmonics Spectrum analysis

A. CASE 1: BALANCED SAG OF 0.35 pu

The performance of the DFIG when the system is subjected to balanced sag of 0.35 pu of the supply voltage. The measured signals in response to the balanced voltage sag are shown in Fig. 7 and Fig. 8. The fault is applied for 100 ms for 5 cycles at 50Hz frequency. When a grid fault occurs, DVR injects series resistance and compensation voltage which adds a voltage drop at the machine terminals as shown in Fig. 7(b). DFIG wind turbine maintains normal operating condition with constant terminal voltage consequently. The Fig. 7(a) compensated using the combined Feed-Forward and Feed-Back control (CFFFB) shows the load voltage in pu in Fig. 7(b) and DVR injection voltage in Volts in Fig. 7(c).

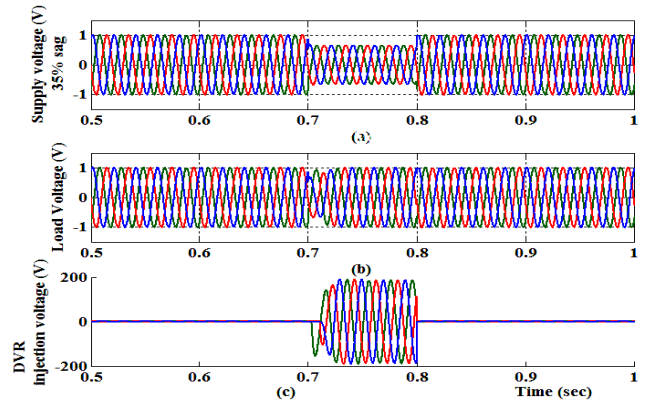


FIGURE 7. DVR using CFFFB control: (a) supply voltage with 35 % balanced sag in pu, (b) load voltage in pu, and (c) DVR injection voltage in Volts.

Fig. 8(a) shows the active power during the .35 pu balanced sag, Fig. 8(b) shows the reactive power, Fig. 8(c) shows the rotor speed control, Fig. 8(d) shows the DC-link voltage, Fig. 8(e) shows the stator current and Fig. 8 (f) shows the rotor current after series compensation during balanced fault condition.

Without any series compensation, the active power injected into the grid with DFIG is almost zero and therefore mechanical power cannot be converted into electrical power leading to high stress in the mechanical system thereby increasing the generator rotor speed. But utilizing DVR, the active power is delivered to the grid as shown in Fig. 8(a) and rotor speed is maintained as shown in Fig. 8(c), thereby maintain the generator in equilibrium condition. Therefore DVR provides smooth power evacuation during fault conditions.

DVR injects voltage in series as shown in Fig. 8(c) to maintain the stator voltage of the DFIG during faults. As the threshold values of rotor current and DC-link voltage are mentioned to ensure efficient FRT capability. The threshold value of the rotor current during fault is 1.5 pu to 2 pu values. Also, the DC-link voltage rating is 1150 V and its threshold value is 1.35 pu. The simulation results show a compliance of these standards. The recovery time of these values are well within the recovery limits as shown in the grid code curves of Fig. 1(a) and Fig. 1(b). The simulation results shows that the DVR based series compensation using CFFFB control works effectively to prevent the DFIG wind turbine from transient voltages and currents.

B. CASE 2: UNBALANCED SAG OF 0.35 pu (SINGLE LINE TO GROUND FAULT, 1LG)

The performance of the DFIG when the system is subjected to unbalanced sag of 0.35 pu of the supply voltage compensated using the combined Feed-Forward and Feed-Back control (CFFFB) is shown. The simulation is carried out when the system is subject to single line to ground fault for 100 ms between 0.7 to 0.8 sec for 5 cycles at 50Hz frequency. The Fig. 9 (a) shows the unbalanced sag in voltage with single phase to ground fault (1LG). The load voltage in pu is shown

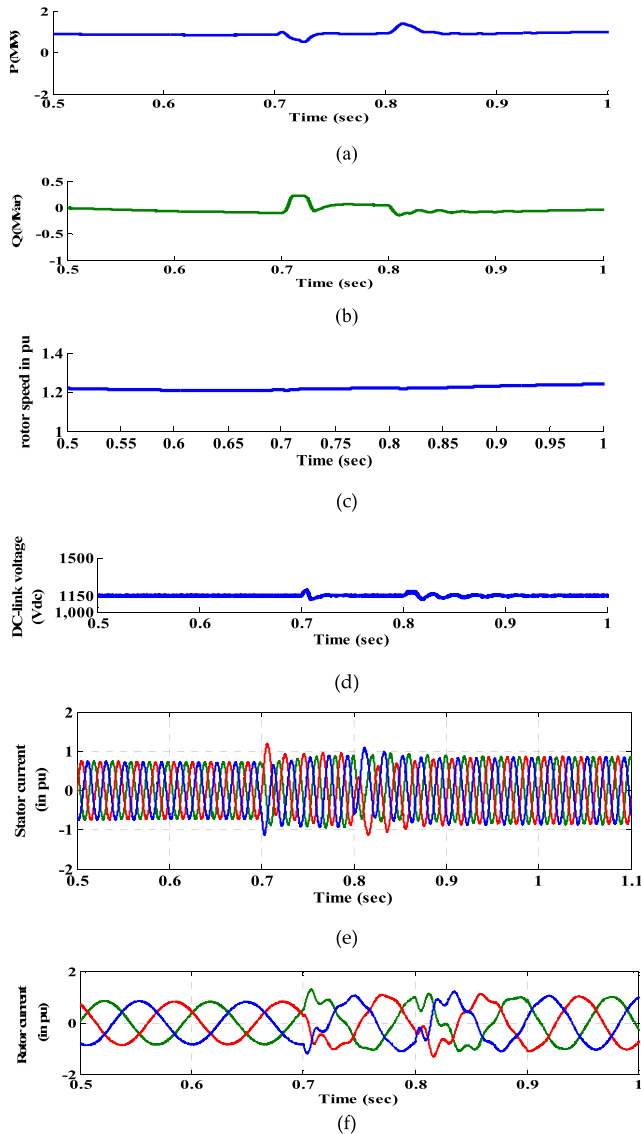


FIGURE 8. (a) Active Power of DFIG with CFFFB control DVR with 35 % balanced sag in pu. (b) Reactive Power of DFIG with CFFFB control DVR with 35 % balanced sag in pu. (c) Rotor speed control of DFIG with CFFFB controlled DVR with 35 % balanced sag in pu. (d) DC-link voltage with CFFFB controlled DVR with 35 % balanced sag in pu. (e) Stator current (GSC current) of DFIG with CFFFB controlled DVR with 35 % balanced sag in pu. (f) Rotor current (RSC current) of DFIG with CFFFB controlled DVR with 35 % balanced sag in pu.

in Fig. 9 (b) and DVR injection voltage in Fig. 10 (c). Fig. 10 (a) shows the active power during the .35 pu unbalanced sag, Fig. 10 (b) shows the reactive power, Fig. 10 (c) shows the rotor speed control, Fig. 10 (d) shows the DC-link voltage, Fig. 10 (e) shows the stator current and Fig. 10 (f) shows the rotor current after series compensation during unbalanced fault condition.

The active power injected into the grid during the fault by DFIG, without series compensation, is almost zero, therefore, the mechanical power cannot be converted into electrical power leading to very high stresses on the mechanical system and increasing the generator rotor speed. By employing DVR,

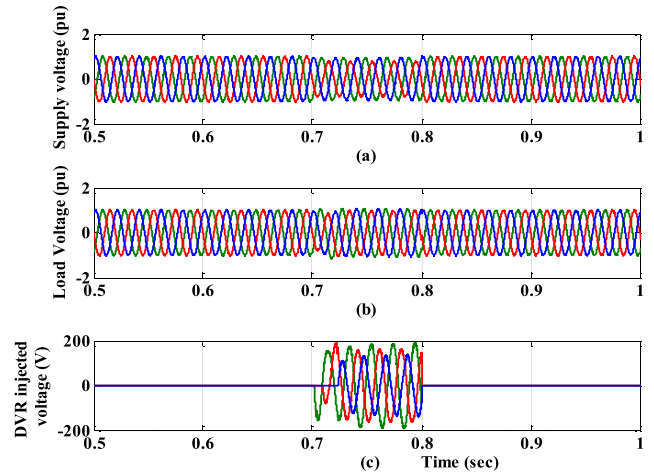


FIGURE 9. DVR using CFFFB control: (a) supply voltage with 35 % unbalanced sag of Phase A (in red) in pu, (b) load voltage in pu, and (c) DVR injection voltage in Volts.

the DFIG wind turbine is able to deliver active power to the grid and keep the generator in an equilibrium condition, as stated in Fig. 8 (a) and Fig. 10 (a). Thereby the active power of DFIG is maintained constant at 1.5 MW even during fault showing a smooth power evacuation of DFIG.

The voltages are injected in series to maintain the stator voltage of the DFIG during the fault using the DVR based series voltage compensation. Overvoltage can be observed on the DC-link of DFIG even up to 1.5 pu without employing DVR. The simulation results in Fig. 8 (d) and Fig. 10 (d) shows effective DC-link voltage control. Also the effectiveness of the proposed series grid interface scheme to isolate the wind turbine from the grid faults to prevent any transient currents or voltages in the DFIG. The rotor speed in Fig. 10 (c) is maintained at 1.2 pu. The series injection using DVR isolated the wind turbine from the asymmetrical faults as shown in Fig. 9 (c).

It takes minimum 4 cycles after the fault occurrence to recover to stable condition. Also the stator and rotor current do not have much over-current values and are well within the threshold limits.

C. CASE 3: SHORT-CIRCUIT FAULT (THREE LINES TO GROUND FAULT, 3LG)

Three phase to ground short-circuit fault between 0.7 to 0.8 sec and the supply voltage is shown in Fig. 11(a) compensated using the combined Feed-Forward and Feed-Back control (CFFFB) shows the load voltage in pu in Fig. 11 (b) and DVR injection voltage in Volts in Fig. 11 (c). Fig. 12 (a) shows the active power, Fig. 13 (b) shows the reactive power, Fig. 12 (c) shows the rotor speed control, Fig. 12 (d) shows the DC-link voltage, Fig. 12 (e) shows the stator current and Fig. 12 (f) shows the rotor current after series compensation during unbalanced fault condition.

The injection of reactive power in Fig. 12(b) shows that the DVR injects 0.5 to 0.3 MVar of reactive power during faults. The DVR uses a voltage source converter to inject series

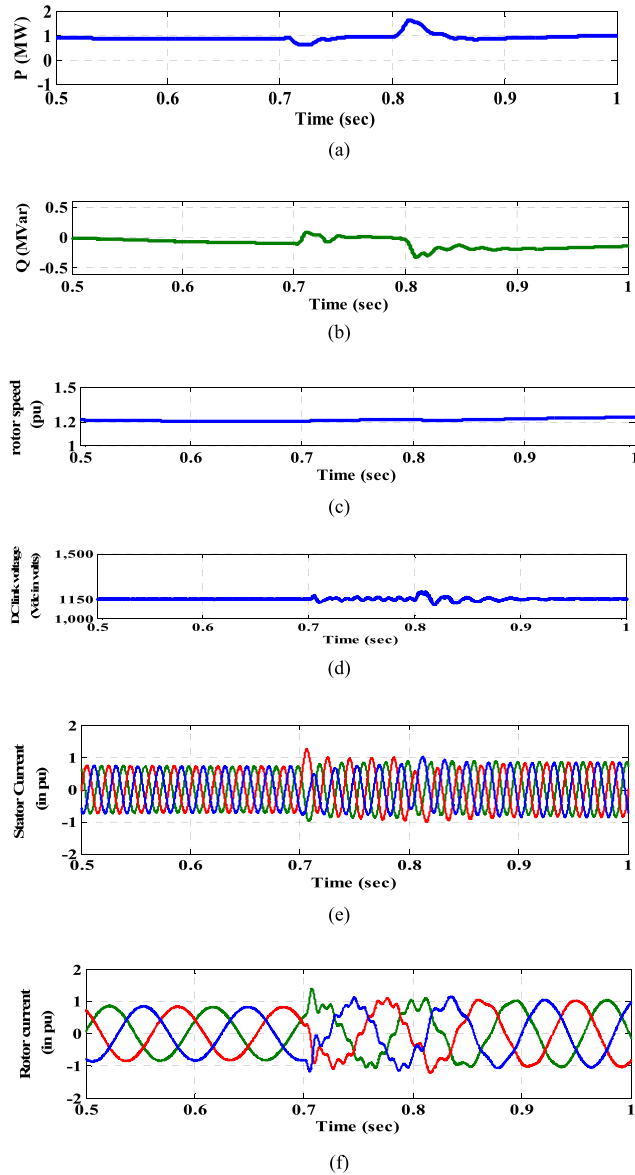


FIGURE 10. (a) Active Power of DFIG with CFFFB control DVR with 35 % unbalanced sag in pu. (b) Reactive Power of DFIG with CFFFB control DVR with 35 % unbalanced sag in pu. (c) Rotor speed control of DFIG with CFFFB controlled DVR with 35 % unbalanced sag in pu. (d) DC-link voltage with CFFFB controlled DVR with 35 % unbalanced sag in pu. (e) Stator current (GSC current) of DFIG with CFFFB controlled DVR with 35 % unbalanced sag in pu. (f) Rotor current (RSC current) of DFIG with CFFFB controlled DVR with 35 % unbalanced sag in pu.

controlled voltage through series transformer. In other words, the DVR system does not change its control structure during different voltage dips. Furthermore, it allows the active and reactive supporting currents to be injected from wind farm to the grid during fault conditions which makes it flexible to fulfill different grid codes. The combined Feed-forward and Feed-back (CFFFB) control is a combination of Feed-forward and PI based Feedback control. The PI regulator is employed to calculate the difference and to compensate the voltage drop through the DVR components.

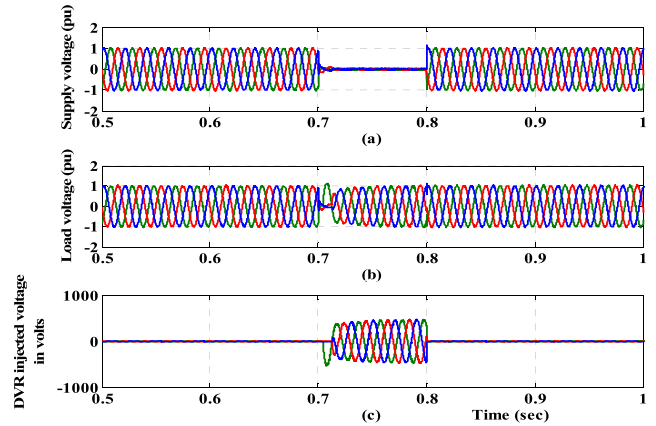


FIGURE 11. DVR using CFFFB control: (a) supply voltage with short circuit three phase to ground fault in pu, (b) load voltage in pu, and (c) DVR injection voltage in Volts.

TABLE 2. Harmonic mitigation using feed forward and CFFFB control.

| THD% values | DVR with Feed forward control | DVR with CFFFB control |
|----------------|-------------------------------|------------------------|
| Supply voltage | 30 % | 30% |
| Supply current | 5.18% | 4.04% |
| Load voltage | 5.24% | 4.47% |
| Load current | 5.18% | 4.04% |

TABLE 3. Performance comparison of feed forward and CFFFB control.

| | DVR with Feed forward control | DVR with CFFFB control |
|-----------------------|---|--|
| Operating frame | Synchronous frame (dq) | Synchronous frame (dq) |
| Digital operation | 2 dq operations | 6 dq operations |
| Tuning | - | K_p, K_i |
| Stability | Unstable for negative sequence operations | Stable |
| Robustness | Does not allow dynamics | Robust to dynamic changes |
| Number of controllers | - | 1 PI control |
| complexity | Very simple | Moderate complexity (require PI gain values, $K_p=0.1, K_i=0.35$) |

The DC-link voltage control in DVR shows that the sudden peak occurring in the dc-link due to sudden voltage drop is below the threshold value of 1.35 pu as shown in Fig. 12 (d). The Fig. 12 (e) and Fig.12 (f) shows that the stator current and rotor currents do not have any over currents above the threshold limits. They take 4 cycles to settle down after slight oscillations due to sudden removal of DVR. Thereby these results confirm the effective operation of DVR using CFFFB control.

The three phase to ground fault or the short-circuit fault is the worst condition during faults and requires the maximum support. DVR can also provide steady-state operations like the load flow control and voltage control. It can also provide additional operations like SSR damping and power system oscillation damping. The parameters of the DFIG and DVR utilized in the simulation are given in Table 1.

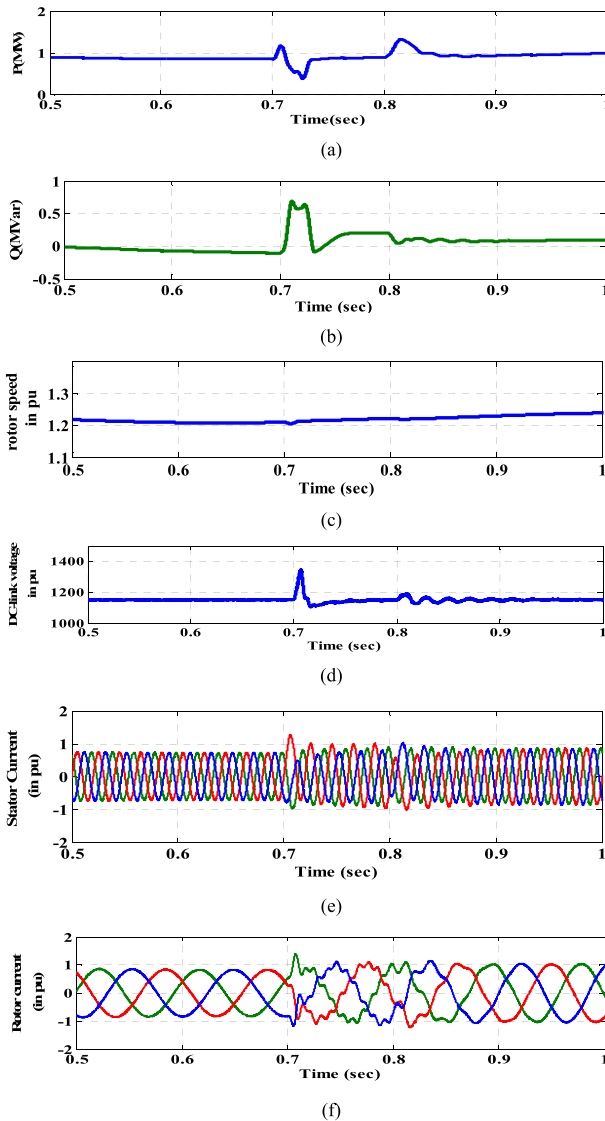


FIGURE 12. (a) Active Power of DFIG with CFFFB control DVR with short circuit three phase to ground fault in pu. (b) Reactive Power of DFIG with CFFFB control DVR with short circuit three phase to ground fault in pu (c) Rotor speed control of DFIG with CFFFB controlled DVR with short circuit three phase to ground fault in pu. (d) DC-link voltage with CFFFB controlled DVR with short circuit three phase to ground fault in pu. (e) Stator current (GSC current) of DFIG with CFFFB controlled DVR with short circuit three phase to ground fault in pu. (f) Rotor current (RSC current) of DFIG with CFFFB controlled DVR with short circuit three phase to ground fault in pu.

D. CASE 4: HARMONICS SPECTRUM ANALYSIS

Harmonics have great negative impacts to the system and most grid disturbances are accompanied with harmonics. Fig. 13 shows the harmonic spectrum of DVR using conventional Feed Forward control and the harmonic spectrum of DVR with CFFFB control is shown in Fig. 14. The CFFFB control based DVR shows lower harmonic distortion within the IEEE 519 standards [35]. The comparison shown in Table 2 shows a significant improvement in the performance of DVR using the PI feedback based CFFFB control. DVR complies to operate within the acceptable limits of THD%. The THD% of DVR without any control is 15.65%, whereas

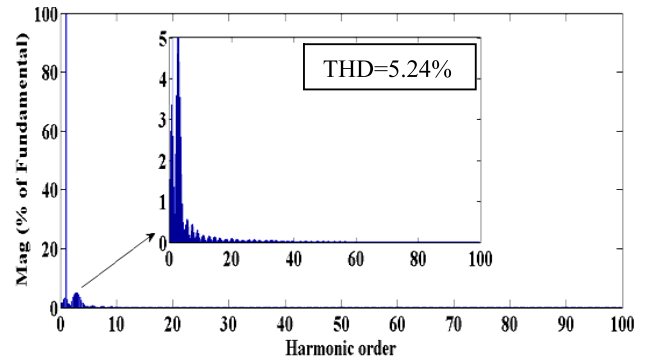


FIGURE 13. Harmonic spectrum of DVR Load voltage with Feed Forward control shows THD=5.24 %.

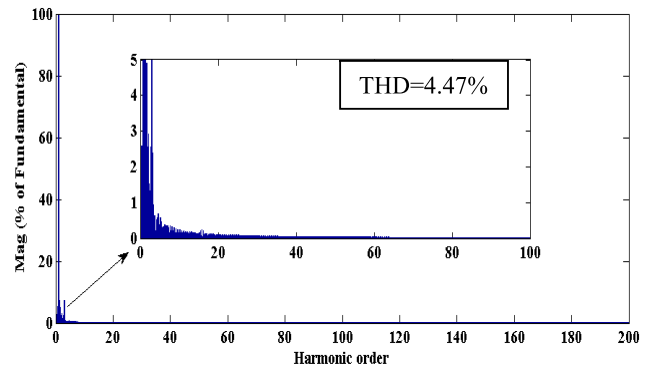


FIGURE 14. Harmonic spectrum of DVR Load voltage with CFFFB control shows THD=4.47 %.

using Feed Forward control it is 5.24% and it is improved by using CFFFB control to 4.47%. The comparison of the harmonic mitigation using the conventional Feed Forward control and the Combined Feed Forward and Feed Back control (CFFFB) is shown in Table 2.

The results and discussion conclude that the improvements in terminal voltage, stator current, rotor current, DC-link voltage are analyzed. Smooth active power evacuation of 1.5 MW power of DFIG is analyzed. Reactive power support during balanced, unbalanced and short-circuit fault conditions are observed. Improvement in harmonic mitigation using the CFFFB control and the operation of DVR for effective FRT capability operation of DFIG based wind turbines during fault is analyzed. The improvement in harmonic mitigation is observed in the harmonic spectrum analysis shown in Fig.13 and Fig.14. The comparison of the performance of the conventional Feed Forward control and the Combined Feed Forward and Feed Back control (CFFFB) is shown in Table 3.

V. CONCLUSION

This paper investigates the performance of DVR with combined Feed-Forward and Feed-Back control for the FRT capability improvement in DFIG based wind turbines. Series compensation scheme using DVR proves to be very effective with good reactive power compensation scheme, voltage control and power flow control. The performance comparison suggests that the operation of DVR is a good suit for improving FRT capability in DFIG based variable speed wind turbines as per grid code standards. The investigated

combined Feed Forward and Feed Back (CFFFB) control has many advantages like simplicity with limited controller complexity. The controller is used to investigate the improvement in performance of FRT capability operation in DFIG wind turbine while modifying the voltage control of a DVR. The DVR proves to deliver very good transient voltage control, fault current control and reactive power support. The controller contributes in better harmonic compensation compared to conventional control as per IEEE 519 standards. The simulation results performed using a 1.5 MW DFIG based wind turbine connected to electrical grid show better performance of DVR with the combined Feed-Forward and Feed-Back control for improving the FRT capability of DFIG based wind turbines.

ACKNOWLEDGMENT

The authors would like to thank the management of VIT University for the support in carrying out this research work. Further, the authors also extended gratitude to the Power Quality Research, Universiti Tenaga Nasional, Malaysia, for providing technical information and also the financial assistance for the project for its current dissemination.

REFERENCES

- [1] R. A. J. Amalorpavaraj, K. Palanisamy, S. Umashankar, and A. D. Thirumorthy, "Power quality improvement of grid connected wind farms through voltage restoration using dynamic voltage restorer," *Int. J. Renew. Energy Res.*, vol. 6, no. 1, pp. 53–60, Mar. 2016.
- [2] R. A. J. Amalorpavaraj, P. Kaliannan, and U. Subramaniam, "Improved fault ride through capability of DFIG based wind turbines using synchronous reference frame control based dynamic voltage restorer," *ISA Trans.*, vol. 70, no. 1, pp. 465–474, Jul. 2017.
- [3] J. Morren and S. W. H. D. Haan, "Ridethrough of wind turbines with doubly-fed induction generator during a voltage dip," *IEEE Trans. Energy Convers.*, vol. 20, no. 2, pp. 435–441, Jun. 2005.
- [4] L. Holdsworth, X. G. Wu, J. B. Ekanayake, and N. Jenkins, "Comparison of fixed speed and doubly-fed induction wind turbines during power system disturbances," *IEE Proc.-Gen. Transmiss. Distrib.*, vol. 150, no. 3, pp. 343–352, May 2003.
- [5] A. D. Hansen and G. Michalke, "Fault ride-through capability of DFIG wind turbines," *Renew. Energy*, vol. 32, no. 9, pp. 1594–1610, Jul. 2007.
- [6] G. Pannell, B. Zahawi, D. J. Atkinson, and P. Missailidis, "Evaluation of the performance of a DC-link brake Chopper as a DFIG low-voltage fault-ride-through device," *IEEE Trans. Energy Convers.*, vol. 28, no. 3, pp. 535–542, Sep. 2013.
- [7] A. Kirakosyan, M. S. El Moursi, P. Kanjiya, and V. Khadkikar, "A nine switch converter-based fault ride through topology for wind turbine applications," *IEEE Trans. Power Del.*, vol. 31, no. 4, pp. 1757–1766, Aug. 2016.
- [8] J. J. Justo, M. Francis, and J. W. Jung, "Enhanced crowbarless FRT strategy for DFIG based wind turbines under three-phase voltage dip," *Electr. Power Syst. Res.*, vol. 142, pp. 215–226, Jan. 2017.
- [9] C. Feltes, H. Wrede, F. W. Koch, and I. Erlich, "Enhanced fault ride-through method for wind farms connected to the grid through VSC-based HVDC transmission," *IEEE Trans. Power Syst.*, vol. 24, no. 3, pp. 1537–1546, Aug. 2009.
- [10] B. B. Ambati, P. Kanjiya, and V. Khadkikar, "A low component count series voltage compensation scheme for DFIG WTs to enhance fault ride-through capability," *IEEE Trans. Energy Convers.*, vol. 30, no. 1, pp. 208–217, Mar. 2015.
- [11] M. K. Döoğlu, A. B. Arsoy, and U. Güvenç, "Application of STATCOM-supercapacitor for low-voltage ride-through capability in DFIG-based wind farm," *Neural Comput. Appl.*, vol. 28, no. 9, pp. 2665–2674, 2017.
- [12] M. Molinas, J. A. Suul, and T. Undeland, "Low voltage ride through of wind farms with cage generators: STATCOM versus SVC," *IEEE Trans. Power Electron.*, vol. 23, no. 3, pp. 1104–1117, May 2008.
- [13] C. Wessels, F. Gebhardt, and F. W. Fuchs, "Fault ride-through of a DFIG wind turbine using a dynamic voltage restorer during symmetrical and asymmetrical grid faults," *IEEE Trans. Power Electron.*, vol. 26, no. 3, pp. 807–815, Mar. 2011.
- [14] D. Ramirez, S. Martinez, C. A. Platero, F. Blazquez, and R. M. de Castro, "Low-voltage ride-through capability for wind generators based on dynamic voltage restorers," *IEEE Trans. Energy Convers.*, vol. 26, no. 1, pp. 195–203, Mar. 2011.
- [15] S. Alaraifi, A. Moawwad, M. S. El Moursi, and V. Khadkikar, "Voltage booster schemes for fault ride-through enhancement of variable speed wind turbines," *IEEE Trans. Sustain. Energy*, vol. 4, no. 4, pp. 1071–1081, Oct. 2013.
- [16] A. O. Ibrahim, T. H. Nguyen, D. C. Lee, and S. C. Kim, "A fault ride-through technique of DFIG wind turbine systems using dynamic voltage restorers," *IEEE Trans. Energy Convers.*, vol. 26, no. 3, pp. 871–882, Sep. 2011.
- [17] M. Farhadi-Kangarlu, E. Babaei, and F. Blaabjerg, "A comprehensive review of dynamic voltage restorers," *Int. J. Electr. Power, Energy Syst.*, vol. 30, no. 92, pp. 136–155, Nov. 2017.
- [18] Y. W. Li, F. Blaabjerg, D. M. Vilathgamuwa, and P. C. Loh, "Design and comparison of high performance stationary-frame controllers for DVR implementation," *IEEE Trans. Power Electron.*, vol. 22, no. 2, pp. 602–612, Mar. 2007.
- [19] Y. W. Li, D. M. Vilathgamuwa, F. Blaabjerg, and P. C. Loh, "A robust control scheme for medium-voltage-level DVR implementation," *IEEE Trans. Ind. Electron.*, vol. 54, no. 4, pp. 2249–2261, Aug. 2007.
- [20] C. K. Sundarabalan and K. Selvi, "Real coded GA optimized fuzzy logic controlled PEMFC based dynamic voltage restorer for reparation of voltage disturbances in distribution system," *Int. J. Hydrogen Energy*, vol. 42, no. 1, pp. 603–613, 2017.
- [21] R. A. J. Amalorpavaraj, *Comparative Analysis of Feed-forward and Synchronous Reference Frame Control Based Dynamic Voltage Restorer* (Lecture Notes in Electrical Engineering). India, Springer, Dec. 2016.
- [22] R. A. J. Amalorpavaraj, P. Kaliannan, and U. Subramaniam, "Testing of low voltage ride through capability compliance of wind turbines—A review," *Int. J. Ambient Energy*, vol. 39, p. 120, Jul. 2017.
- [23] P. Roncero-Sánchez, E. Acha, J. E. Ortega-Calderon, V. Feliu, and A. García-Cerrada, "A versatile control scheme for a dynamic voltage restorer for power-quality improvement," *IEEE Trans. Power Del.*, vol. 24, no. 1, pp. 277–284, Jan. 2009.
- [24] J. Roldán-Pérez, A. García-Cerrada, J. L. Zamora-Macho, P. Roncero-Sánchez, and E. Acha, "Troubleshooting a digital repetitive controller for a versatile dynamic voltage restorer," *Int. J. Electr. Power Energy Syst.*, vol. 57, pp. 105–115, May 2014.
- [25] H. Kim and S.-K. Sul, "Compensation voltage control in dynamic voltage restorers by use of feed forward and state feedback scheme," *IEEE Trans. Power Electron.*, vol. 20, no. 5, pp. 1169–1177, Sep. 2005.
- [26] G. Joos, S. Chen, and L. Lopes, "Closed-loop state variable control of dynamic voltage restorers with fast compensation characteristics," in *Proc. 39th IAS Annu. Meet. IEEE Ind. Appl. Conf. Rec.*, vol. 4, Sep. 2004, pp. 2252–2258.
- [27] M. Sarhangzadeh, S. H. Hosseini, M. B. B. Sharifian, G. B. Gharehpetian, and O. Sarhangzadeh, "Dynamic analysis of DVR implementation based on nonlinear control by IOFL," in *Proc. 24th Can. Conf. Electr. Comput. Eng. (CCECE)*, Niagara Falls, ON, Canada, 2011, pp. 000264–000269.
- [28] P. H. Huang, M. S. El Moursi, W. Xiao, and J. L. Kirtley, Jr., "Novel fault ride-through configuration and transient management scheme for doubly fed induction generator," *IEEE Trans. Energy Convers.*, vol. 28, no. 1, pp. 86–94, Mar. 2013.
- [29] S. Biricik and H. Komurçugil, "Optimized sliding mode control to maximize existence region for single-phase dynamic voltage restorers," *IEEE Trans. Ind. Informat.*, vol. 12, no. 4, pp. 1486–1497, Aug. 2016.
- [30] M. González, V. Cárdenas, L. Morán, and J. Espinoza, "Selecting between linear and nonlinear control in a dynamic voltage restorer," in *Proc. IEEE Power Electron. Specialists Conf. (PESC)*, Jun. 2008, pp. 3867–3872.
- [31] M. González, V. Cárdenas, and G. Espinosa, "Advantages of the passivity based control in dynamic voltage restorers for power quality improvement," *Simul. Model. Pract. Theory*, vol. 47, pp. 221–235, Sep. 2014.
- [32] S. M. Mueyen *et al.*, "Comparative study on transient stability analysis of wind turbine generator system using different drive train models," *IET Renew. Power Gen.*, vol. 1, no. 2, pp. 131–141, Jun. 2007.
- [33] M. Rahimi and M. Parniani, "Dynamic behavior analysis of doubly-fed induction generator wind turbines: the influence of rotor and speed controller parameters," *Int. J. Electr. Power, Energy Syst.*, vol. 32, no. 5, pp. 464–477, 2010.

- [34] A. Patil and A. Thosar, "Steady state and transient stability analysis of wind energy system," in *Proc. 2nd Int. Conf. Control, Instrum., Energy, Commun. (CIEC)*, Kolkata, India, 2016, pp. 250–254.
- [35] A. A. Hussein and M. H. Ali, "Comparison among series compensators for transient stability enhancement of doubly fed induction generator based variable speed wind turbines," *IET Renew. Power Gen.*, vol. 10, no. 1, pp. 116–126, 2016.
- [36] L. Ran, D. Xiang, P. J. Tavner, and S. Yang, "Control of a doubly fed induction generator in a wind turbine during grid fault ride-through," in *Proc. IEEE Power Eng. Soc. Gen. Meet.*, Montreal, QC, Canada, Jun. 2006, pp. 652–662.
- [37] R. Pena, J. C. Clare, and G. M. Asher, "A doubly fed induction generator using back-to-back PWM converters supplying an isolated load from a variable speed wind turbine," *IEE Proc.-Electr. Power Appl.*, vol. 143, no. 5, pp. 380–387, Sep. 1996.



RINI ANN JERIN AMALORPAVARAJ (S'16) received the bachelor's degree in electrical engineering from the Sri Shakthi Institute of Engineering and Technology, Anna University, Chennai, India, in 2012, the master's (Hons.) degree in renewable energy technologies from Karunya University, Coimbatore, India, in 2014. She is currently pursuing the Ph.D. degree in electrical engineering at VIT University, Vellore, India. She has published more than ten papers in various

international journals and conferences and also several book chapters. Her research interests include renewable energy, grid integration, transient stability, fault ride through, FACTS, wind energy, distributed generation, and battery storage. She is a member of several technical bodies, which include the IEEE IES, the IEEE PES, and the IEEE Women in Engineering and Women in Power. She is also involved in peer-review of reputed journals like the IET and Elsevier.



PALANISAMY KALIANNAN received the bachelor's degree in electrical engineering from the KSR College of Technology, India, in 2000, the master's (Hons.) degree in electrical engineering from the Coimbatore Institute of Technology, India, in 2004, and the Ph.D. degree in electrical engineering from VIT University, Vellore, India, in 2013.

He is currently an Associate Professor and the Head of the Energy and Power Electronics Division at VIT University, since 2007. He has authored over 50 scientific papers in referred conference proceedings and international journals in the field of renewable energy, battery storage, and power electronics with particular reference to multilevel converters. He is a certified Energy Auditor by the Bureau of Energy Efficiency. He has taken up various consultant projects in collaboration with TNEB, Southern Railway, the National Institute of Wind Energy, and Danfoss Industries Pvt., Ltd., Chennai, India.



SANJEEVIKUMAR PADMANABAN (M'12–SM'15) received the bachelor's degree in electrical engineering from the University of Madras, India, in 2002, the master's (Hons.) degree in electrical engineering from Pondicherry University, India, in 2006, and the Ph.D. degree in electrical engineering from the University of Bologna, Italy, in 2012, with full comprehensive grant successfully obtained from Ministry of University Research, from the Government of Italy from 2009 to 2011, by securing first rank among International Competition devoted for one foreign Ph.D. scholarship position. His biography was included along with the 2000 Outstanding Intellectuals of the 21st Century-9th Edition-International Biographical Center, Cambridge, U.K., 2015. He was an Associate Professor with VIT University from 2012 to 2013. In 2013, he joined as a Faculty Member the National Institute of Technology, Pondicherry. In 2014, he was invited as a Visiting Researcher by the Department of Electrical Engineering, Qatar University, Qatar, funded by the Qatar National Research Foundation, Government of Qatar.

He continued his research activities with the Dublin Institute of Technology, Ireland, in 2014. He has been an Associate Professor with the Department of Electrical and Electronics Engineering, University of Johannesburg, South Africa, since 2016. He has authored over 150 scientific papers and has received the Best Paper cum the Most Excellence Research Paper Award of IET-SEISCON 2013 IET-CEAT 2016, and five best paper awards from ETAERE 2016 Springer sponsored Lecture Notes in electrical engineering book chapters.

Dr. Padmanaban serves as an Editor/Associate Editor/Editorial Board Member of over 150 refereed journal in particular the IEEE TRANSACTION ON POWER ELECTRONICS, the *IET Power Electronics*, the *IET Renewable Power Generation*, the *IET Generation, Transmission and Distribution*, and IEEE ACCESS. He was invited as an Honorary Program Committee/Technical Committee/Steering Committee Member/Chair of over 4000 various international and national conferences in India and abroad, in particular, the IEEE.



UMASHANKAR SUBRAMANIAM (M'11) received the bachelor's degree in electrical engineering from the Government College of Technology, Coimbatore, India, in 2001, the master's (Hons.) degree in power electronics and drives, and the Ph.D. degree in electrical engineering from VIT University, Vellore, India, in 2004 and 2013, respectively.

He is currently with the School of Electrical Engineering as an Associate Professor at VIT University. He has over 13 years of teaching, research, and industrial research and development experience. He is a member of IEEE-IAS, IEEE-PES, IACSIT, IDES, and ISTE. He has published more than 100 research papers in national and international journals and conferences and ten books/chapters.



VIGNA K. RAMACHANDARAMURTHY (SM'12) received the Ph.D. degree in electrical engineering from the University of Manchester Institute of Science and Technology in 2001. He is currently a Professor with the Institute of Power Engineering, UNITEN. He has successfully supervised and graduated over 100 Ph.D. students, with many receiving distinction. His area of interest includes power systems related studies, renewable energy, energy storage, power quality, electric vehicle, and

rural electrification. He is the currently a Principal Consultant for Malaysia's biggest electrical utility, Tenaga Nasional Berhad, and has completed over 200 projects in renewable energy. He has also developed several technical guidelines for distributed generation in Malaysia. In 2008, he received the IET Mike Sargeant Award for career achievement. In 2009, he received the Institution of Engineers Malaysia (IEM) Young Engineers Award. He has served as the IET Malaysia Chairman, the IET Council Member, IEM Council Member, the IET Younger Members Board representing West Asia, as an International Professional Registration Advisor, an Interviewer and the Convenor for Chartered Engineering, U.K., Malaysia. He is also a Chartered Engineer registered with the Engineering Council, U.K., and a Professional Engineer registered with the Board of Engineers Malaysia.